High-efficiency terahertz pulse generation via optical rectification by suppressing stimulated Raman scattering process

Masaya Nagai,* Eiichi Matsubara, and Masaaki Ashida

Graduate School of Engineering Science, Osaka University, 1-3 Machikaneyama-cho, Toyonaka, Osaka 560-8531, Japan

mnagai@mp.es.osaka-u.ac.jp

Abstract: We experimentally demonstrate high-efficiency terahertz pulse generation via optical rectification in $LiNbO_3$. The spectral broadening of an excitation pulse via the stimulated Raman scattering process coincides with high-efficiency terahertz pulse generation, which enhances undesired stretching of the excitation pulse owing to the very high group velocity dispersion in $LiNbO_3$. We avoid this by the bandwidth control of the excitation pulse and achieve the highest reported efficiency of 0.21% for energy conversion into a THz pulse.

OCIS codes: (190.4410) Nonlinear optics, parametric processes; (190.7110) Ultrafast nonlinear optics; (300.6495) Spectroscopy, terahertz.

References and links

1. K. Sakai, ed., *Terahertz Optoelectronics* (Springer, Berlin, 2005).
2. M. Tonouchi, "Cutting-edge terahertz technology," Nat. Photonics **1**(2), 97–105 (2007).
3. A. Rice, Y. Jin, X. F. Ma, X.-C. Zhang, D. Bliss, J. Larkin, and M. Alexander, "Terahertz optical rectification from 110 zinc-blende crystals," Appl. Phys. Lett. **64**(11), 1324–1326 (1994).
4. M. Nagai, K. Tanaka, H. Ohtake, T. Bessho, T. Sugiura, T. Hirosumi, and M. Yoshida, "Generation and detection of terahertz radiation by electro-optical process in GaAs using 1.56μm fiber laser pulses," Appl. Phys. Lett. **85**(18), 3974–3976 (2004).
5. F. Blanchard, L. Razzari, H. C. Bandulet, G. Sharma, R. Morandotti, J. C. Kieffer, T. Ozaki, M. Reid, H. F. Tiedje, H. K. Haugen, and F. A. Hegmann, "Generation of 1.5 μJ single-cycle terahertz pulses by optical rectification from a large aperture ZnTe crystal," Opt. Express **15**(20), 13212–13220 (2007).
6. J. Hebling, G. Almási, I. Kozma, and J. Kuhl, "Velocity matching by pulse front tilting for large area THz-pulse generation," Opt. Express **10**(21), 1161–1166 (2002).
7. J. Hebling, A. G. Stepanov, G. Almási, B. Bartal, and J. Kuhl, "Tunable THz pulse generation by optical rectification of ultrashort laser pulses with tilted pulse fronts," Appl. Phys. B **78**, 593–599 (2004).
8. A. Stepanov, J. Kuhl, I. Kozma, E. Riedle, G. Almási, and J. Hebling, "Scaling up the energy of THz pulses created by optical rectification," Opt. Express **13**(15), 5762–5768 (2005).
9. K.-L. Yeh, M. C. Hoffmann, J. Hebling, and K. A. Nelson, "Generation of 10μJ ultrashort terahertz pulses by optical rectification," Appl. Phys. Lett. **90**(17), 171121 (2007).
10. J. Hebling, K.-L. Yeh, M. C. Hoffmann, B. Bartal, and K. A. Nelson, "Generation of high-power terahertz pulses by tilted-pulse-front excitation and their application possibilities," J. Opt. Soc. Am. B **25**(7), B6–B19 (2008).
11. A. G. Stepanov, S. Henin, Y. Petit, L. Bonacina, J. Kasparian, and J.-P. Wolf, "Mobile source of high-energy single-cycle terahertz pulses," Appl. Phys. B **101**(1-2), 11–14 (2010).
12. H. Hirori, A. Doi, F. Blanchard, and K. Tanaka, "Single-cycle terahertz pulses with amplitudes exceeding 1 MV/cm generated by optical rectification in $LiNbO_3$," Appl. Phys. Lett. **98**(9), 091106 (2011).
13. E. Abraham, Y. Ohgi, M. A. Minami, M. Jewariya, M. Nagai, T. Araki, and T. Yasui, "Real-time line projection for fast terahertz spectral computed tomography," Opt. Lett. **36**(11), 2119–2121 (2011).
14. F. Blanchard, A. Doi, T. Tanaka, H. Hirori, H. Tanaka, Y. Kadoya, and K. Tanaka, "Real-time terahertz near-field microscope," Opt. Express **19**(9), 8277–8284 (2011).
15. K. Tanaka, H. Hirori, and M. Nagai, "THz nonlinear spectroscopy of solids," IEEE Trans. Terahertz Sci. Technol. **1**(1), 301–312 (2011).
16. S. Fleischer, Y. Zhou, R. W. Field, and K. A. Nelson, "Molecular orientation and alignment by intense single-cycle THz pulses," Phys. Rev. Lett. **107**(16), 163603 (2011).
17. J. A. Fülöp, L. Pálfalvi, G. Almási, and J. Hebling, "Design of high-energy terahertz sources based on optical rectification," Opt. Express **18**(12), 12311–12327 (2010).
18. J. A. Fülöp, L. Pálfalvi, Z Ollmann, and J. Hebling, "Towards generation of mJ-level ultrashort THz pulses by optical rectification," Opt. Express **19**(16), 15090–15097 (2011).

#162439 - $15.00 USD Received 2 Feb 2012; revised 1 Mar 2012; accepted 1 Mar 2012; published 5 Mar 2012

19. C. Langrock, M. M. Fejer, I. Hartl, and M. E. Fermann, "Generation of octave-spanning spectra inside reverse-photon-exchanged periodically poled lithium niobate waveguides," Opt. Lett. **32**(17), 2478–2480 (2007).
20. C. R. Phillips, C. Langrock, J. S. Pelc, M. M. Fejer, I. Hartl, and M. E. Fermann, "Supercontinuum generation in quasi-phasematched waveguides," Opt. Express **19**(20), 18754–18773 (2011).
21. A. Ridah, M. D. Fontana, and P. Bourson, "Temperature dependence of the Raman modes in $LiNbO_3$ and mechanism of the phase transition," Phys. Rev. B **56**(10), 5967–5973 (1997).
22. E. Matsubara, T. Sekikawa, and M. Yamashita, "Generation of ultrashort optical pulses using multiple coherent anti-Stokes Raman scattering in a crystal at room temperature," Appl. Phys. Lett. **92**(7), 071104 (2008).
23. M. Jewariya, M. Nagai, and K. Tanaka, "Enhancement of terahertz wave generation by cascaded $\chi^{(2)}$ processes in $LiNbO_3$," J. Opt. Soc. Am. B **26**(9), A101–A106 (2009).
24. Q. Wu and X.-C. Zhang, "Ultrafast electro-optic field sensors," Appl. Phys. Lett. **68**(12), 1604–1606 (1996).
25. A. G. Stepanov, A. A. Mel'nikov, V. O. Kompanets, and S. V. Chekalin, "Spectral modification of femtosecond laser pulses in the process of highly efficient generation of terahertz radiation via optical rectification," JETP Lett. **85**(5), 227–230 (2007).
26. M. Nagai, M. Jewariya, Y. Ichikawa, H. Ohtake, T. Sugiura, Y. Uehara, and K. Tanaka, "Broadband and high power terahertz pulse generation beyond excitation bandwidth limitation via χ^2 cascaded processes in LiNbO3," Opt. Express **17**(14), 11543–11549 (2009).
27. E. D. Palik, ed., *Handbook of Optical Constants of Solids* (Academic Press, New York, 1985)
28. M. C. Hoffmann, K.-L. Yeh, J. Hebling, and K. A. Nelson, "Efficient terahertz generation by optical rectification at 1035 nm," Opt. Express **15**(18), 11706–11713 (2007).
29. M. C. Hoffmann, K.-L. Yeh, H. Y. Hwang, T. S. Sosnowski, B. S. Prall, J. Hebling, and K. A. Nelson, "Fiber laser pumped high average power single-cycle terahertz pulse source," Appl. Phys. Lett. **93**(14), 141107 (2008).
30. J. A. Fülöp, L. Pálfalvi, S. Klingebiel, G. Almási, F. Krausz, S. Karsch, and J. Hebling, "Generation of sub-mJ terahertz pulses by optical rectification," Opt. Lett. **37**(4), 557–559 (2012).

1. Introduction

Coherent few-cycle terahertz (THz) pulses have various potential uses in a range of applications in the fields of physics, chemistry, and biology [1, 2]. Recently, the generation of extremely intense THz pulses has been achieved via the nonresonant optical rectification process. Quadric $\chi^{(2)}$ materials satisfying the phase-matching condition enable intense THz pulse generation even with intense optical excitation [3–5]. In particular, the tilted pulse front excitation of high-$\chi^{(2)}$ media such as $LiNbO_3$ enables very efficient THz pulse generation, in which the pulse satisfies the phase matching condition in a non-collinear geometry. This technique was proposed by Hebling and associates [6, 7] and has been experimentally demonstrated by many researchers [8–10]. The highest reported output pulse energy is 50 μJ [11] and the highest reported electric field exceeds 1 MV/cm [12]. These THz sources are expected to enable rapid imaging [13, 14] and lead to new methods of nonlinear spectroscopy in the THz frequency region [15, 16].

The advantage of this THz pulse generation technique is its high efficiency. Since the output pulse energy of a THz pulse via the $\chi^{(2)}$ process is proportional to the square of the input pulse energy, the intense optical excitation pulse and long interaction length in a $\chi^{(2)}$ crystal can enhance the conversion efficiency. The input pulse energy and interaction length are practically limited by multiphoton absorption and group velocity dispersion (GVD), respectively. Numerical simulations indicate energy conversion efficiency approaching a few percent [17, 18]. However, the experimentally reported energy conversion efficiency has been less than 0.1% (10^{-3}), even using an intense pulse from a Ti:sapphire amplifier system [10, 12]. Here, we propose that instantaneous $\chi^{(3)}$ nonlinear processes, including the stimulated Raman scattering (SRS) process, coinciding with the $\chi^{(2)}$ process, reduce the efficiency of THz pulse generation. In general, an efficient cascaded $\chi^{(2)}$ process is equivalent to an effective $\chi^{(3)}$ process and has been used for ultrashort pulse shaping in a periodic-poled $LiNbO_3$ waveguide via second harmonic generation [19]. In this case, the cascaded $\chi^{(2)}$ and $\chi^{(3)}$ phase modulations are of opposite sign and have a comparable magnitude, and another third-order nonlinearity originating from SRS affects the spectral modulation of a broadband excitation pulse [20]. For optical rectification, SRS may coincide with the $\chi^{(2)}$ process when using a conventional Ti:sapphire laser with < 100 fs pulse duration whose bandwidth covers the lowest TO_1 (A) phonon frequency (7.6 THz) [21]. Actually the spectral broadening of an excitation pulse via SRS has been reported in $LiNbO_3$ [22], as well as undesired energy dissipation. This may cause the temporal stretching of an excitation pulse due to the very high

#162439 - $15.00 USD Received 2 Feb 2012; revised 1 Mar 2012; accepted 1 Mar 2012; published 5 Mar 2012

GVD in $LiNbO_3$, which reduces the efficiency of THz pulse generation. In this study, we control the spectral width of excitation pulses to less than the frequency of the Raman-active phonon mode to suppress the SRS process. As a result, we achieved the highest ever reported conversion efficiency of 0.21% for THz pulse generation.

2. Experimental setup

The experimental setup is almost the same as that in ref [23]. We use optical pulses from an amplified laser system with a repetition rate of 1 kHz, an average power of 580 mW, and a center wavelength of 780 nm (a weighted center frequency of 383.8 THz). We previously demonstrated THz pulse generation using this excitation laser with 150 fs pulse duration and reported a saturated conversion efficiency of 0.08% [23]. In the present study, we tuned the Pockels cell in the cavity of the Ti:sapphire regenerative amplifier for the selective amplification of high-frequency components of the seed laser (femtolite, IMRA America Inc.) and reduced the bandwidth of the amplified pulse to 3.3 THz. This frequency is less than the TO_1 phonon frequency (7.6 THz). The full width at half maximum of the autocorrelation signal is 280 fs, corresponding to a net pulse duration of ~200 fs. This optical beam is split into two for THz pulse generation and detection. We control the excitation pulse front using an gold-coated 2000 lines/mm holographic grating and two lenses, and we inject it onto an emitter with a spot size of 1.5 × 1 mm^2, smaller than that in ref [23], without any damage to the emitter. Such a small spot size suppresses the effect of tilted pulse front distortion [12]. The emitter is a stoichiometric $LiNbO_3$ crystal with a Mg concentration of 1.5%. One surface is cut with an angle of 62° and is antireflection-coated for near-infrared wavelengths. The generated THz pulse is guided using two off-axis parabolic mirrors (50 mm diameter and 50 mm focal length) and the emitter image is transferred onto the detector.

We evaluated the electric field amplitude using an electrooptic (EO) sampling technique. As the EO crystal we used a (110)-oriented GaP crystal with a thickness of L = 0.3 mm. The low EO coefficient (r_{41} = 1 pm/V) and high phonon frequency in GaP enabled the detection of intense and broadband THz radiation. The EO signal caused by a phase shift θ can be easily calibrated using the formula $\Delta I/I = \sin\theta = 2\pi/\lambda\ n_{opt}^3\ r_{41}\ E_{THz}L$, where n_{opt} = 3.2 is the refractive index of GaP at λ = 780 nm [24]. To prevent the saturation of sensitivity, we placed six Si plates in the path of the THz radiation, which acted as attenuation filters with a large reflection loss. We divided the Fourier components of the THz pulse by $2/(n_{THz}-1)\ (e^{i\Delta kL}-1)/i\Delta k$ to compensate for the Frenel loss and phase mismatch Δk in GaP, and obtain the true time evolution of the electric field from the Fourier components below 3.5 THz.

3. Experiments and discussions

Figure 1(a) shows the temporal evolution of the electric field evaluated from the EO signal. The observed electric field is as high as 380 kV/cm. In this measurement, although we used a sampling pulse with a duration of 200 fs, the delay time between the maximum and minimum electric field is only 300 fs. This implies that the temporal profile of the electric field becomes dull. By deconvoluting the sampling pulse, we found that the prospective electric field exceeds 500 kV/cm. Figure 1(b) shows the power spectrum corresponding to Fig. 1(a). In this figure, we show the Fourier components before dividing by the sensitivity factor $2/(n_{THz}-1)\ (e^{i\Delta kL}-1)/i\Delta k$. The weighted center frequency of the emitted THz pulse is estimated to be 1.09 THz. In spite of the longer pulse duration of 200 fs, the spectral bandwidth of the emitted THz pulse is similar to that obtained using a 100 fs excitation pulse.

#162439 - $15.00 USD Received 2 Feb 2012; revised 1 Mar 2012; accepted 1 Mar 2012; published 5 Mar 2012

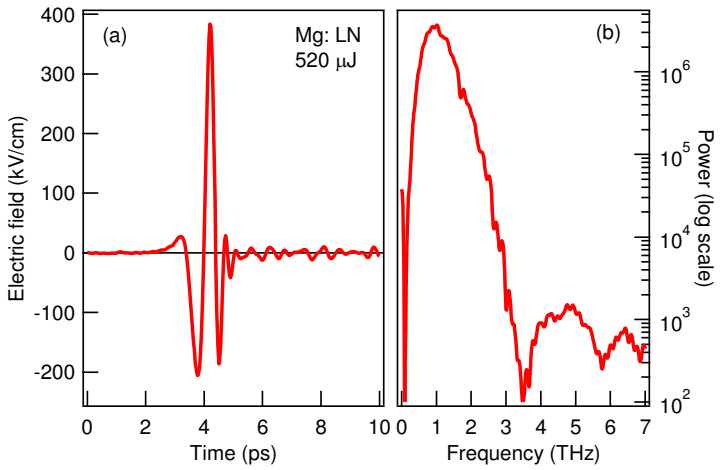

Fig. 1. (a) Temporal profile of THz pulse emitted from Mg-doped $LiNbO_3$ using excitation pulse with duration of 200 fs and pulse energy of 520 μJ. (b) Power spectrum of THz pulse evaluated from temporal profile.

We also evaluated the output pulse energy to be 1.1 μJ using a conventional thermal sensor (PM30, Coherent Inc.). In this measurement, we removed the entire optical component using an optical diffusion filter (a thick Teflon plate) and an optical absorption filter (a thin black polypropylene film). The input pulse energy was measured to be 520 μJ using the same sensor, meaning that the conversion efficiency from these pulse energies reached 0.21%. This value is higher than the previous reported values of less than 0.1% [10, 15].

Fülöp et al. carried out simulations to obtain the THz pulse generation efficiency under various excitation conditions while taking into account the linear dispersion of $LiNbO_3$ and the multiphoton absorption of the excitation pulse [18, 19]. They pointed out that the effective THz generation length which is determined by the stretching of the excitation pulse due to the large GVD in $LiNbO_3$, strongly affects the conversion efficiency, and concluded that the generation efficiency increases when the excitation pulse duration increases to several hundred fs. Their conclusions appear to support our results. However, such a large improvement of the generation efficiency from 0.08% to 0.21% by changing the excitation pulse duration from 150 fs to 200 fs cannot be reproduced by their numerical simulations.

To elucidate the origin of this discrepancy, we measured the spectra of the excitation pulses passing through the $LiNbO_3$ crystal. Figure 2(a) shows the spectra of the excitation pulse before and after passing through the $LiNbO_3$ crystal. The incident pulse energies are 30 μJ (dotted curve) and 520 μJ (solid curve). The weighted center frequency of the original excitation pulse is 383.8 THz. However, the spectrum of the transmitted excitation pulse is shifted to a lower weighted center frequency of 382.1 (374.5) THz for the incident energy of 30 (520) μJ. Such a spectral shift has already been reported in several papers [23, 25, 26] and has been considered as evidence of efficient THz pulse generation; assuming an excitation pulse emitting an intense THz pulse in a lossless nonlinear medium, its frequency shift corresponds to the generation efficiency. Now, let us examine the spectra in Fig. 2 more closely. One can see several characteristic structures in the spectra. In the case of 30 μJ pulse energy, a peak appears at a frequency 7.0 THz lower than the peak frequency of the incident excitation pulse, whereas for 520 μJ pulse energy, one broad peak appears at a center frequency 8.0 THz lower than the peak frequency for the 30 μJ pulse. Such peaks cannot be explained by considering only the $\chi^{(2)}$ processes obtained from numerical simulation even for a lossy nonlinear medium [23].

We postulate that such peaks are due to the SRS process. Figure 2(b) shows the Raman intensity I_R of $LiNbO_3$ at room temperature. The configuration X(ZZ)Y is almost the same as that for THz pulse generation. Four characteristic Raman modes appear at 252, 275, 332, and

#162439 - $15.00 USD Received 2 Feb 2012; revised 1 Mar 2012; accepted 1 Mar 2012; published 5 Mar 2012

632 cm^{-1}, denoted as the A_1 (TO_1), A_1 (TO_2), A_1 (TO_3), and A_1 (TO_4) modes, respectively [21]. We evaluate the complex Raman tensor χ^R, shown in Fig. 2(c), from the Raman spectrum using the relation $I_R \propto \omega \mathrm{Im}[\chi^R]$, assuming the superposition of four Lorentz functions. Since the value of $\chi^{(3)}$ for SRS is partially related to the value of χ^R, Fig. 2(c) implies enhanced SRS for the TO_1 (7.4 THz) and TO_4 (19 THz) modes. The frequency shifts in Fig. 2(a) are almost the same as the frequencies of the TO_1 Raman mode, as shown in Fig. 2(c). Since the energy of the incident excitation pulse is sufficiently large to cause SRS, we consider that the peak for 30 μJ pulse energy originates from the SRS of the TO_1 mode. For the 520 μJ pulse energy, the spectral shape satisfies the complex nonlinear propagation equation including $\chi^{(3)}$ for SRS as shown in Fig. 2(c).

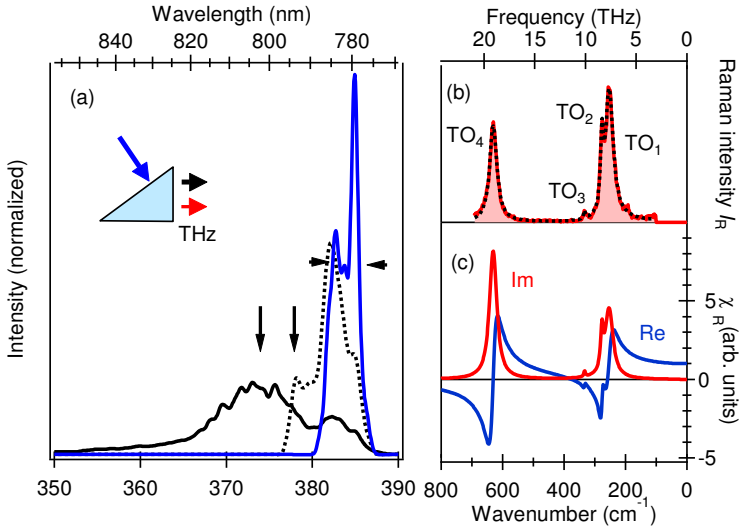

Fig. 2. (a) Optical spectra of excitation pulse (blue curve) and transmitted excitation pulses after passing through $LiNbO_3$ (black curves) when the incident pulse energy is 30 μJ (dotted curve) and 520 μJ (solid curve). These spectra are normalized by their area. (b) Raman intensity I_R of $LiNbO_3$ at room temperature in the X(ZZ)Y configuration. The dashed curve is the fitting with four Lorentz functions. (c) Complex Raman tensor evaluated from Raman spectrum, which originates from the four phonon modes in (b).

The above spectral peaks in the transmitted excitation pulse were more apparent when using a broader-band excitation pulse with 150 fs duration [23]. A sharp peak initially appears at the lowest frequency of the incident pulse spectrum. This behavior is characteristic of spectral modulation via SRS, which greatly reduces the generation efficiency. In the present experiment, the bandwidth of the excitation pulse does not cover the phonon frequency, and the peaks in Fig. 2(a) appear to be outside the spectrum of the incident excitation pulse. To achieve SRS with a narrow-bandwidth excitation pulse, spectral broadening with a different mechanism such as a cascaded $\chi^{(2)}$ process is necessary.

From these findings, we consider the following mechanism for high-efficiency THz pulse generation. Immediately after the excitation pulse is incident to the $LiNbO_3$ crystal, a THz pulse is efficiently generated via optical rectification. The emitted intense THz pulse modulates the phase of the optical excitation pulse, causing a Stokes shift of the excitation pulse with spectral broadening via the cascaded $\chi^{(2)}$ process. This provides a new generation channel for higher-frequency THz components, and further frequency conversion is possible [26]. When the spectral width of the excitation pulse reaches 7.4 THz, it starts to be accompanied by SRS, causing the spectral broadening of the excitation pulse to be accelerated. Such spectral broadening above 7.4 THz does not provide a new generation channel for the THz component, and results in energy loss of the excitation pulse. Furthermore, the very high GVD of 360 fs^2/mm at 780 nm in $LiNbO_3$ [27] causes optical

#162439 - $15.00 USD Received 2 Feb 2012; revised 1 Mar 2012; accepted 1 Mar 2012; published 5 Mar 2012

pulse stretching with a short propagation distance. Consequently, the generation efficiency of the THz pulse becomes saturated. This mechanism is schematically shown in Fig. 3.

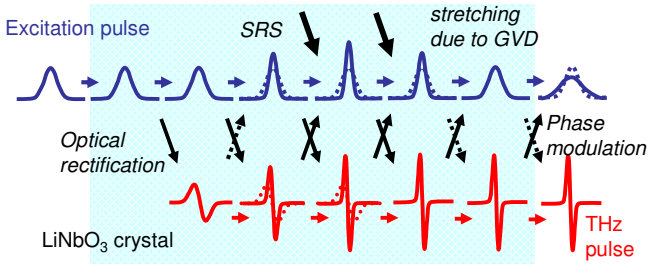

Fig. 3. THz pulse generation coinciding with cascaded $\chi^{(2)}$ process and SRS.

According to our new consideration of the THz generation efficiency, there is another unavoidable factor limiting the efficiency, the SRS process, in addition to the factors considered by Fülöp et al. [18, 19]. Since calibrating the $\chi^{(3)}$ value in $LiNbO_3$ may be challenging [20], there may be considerable uncertainty even if we take into account the SRS effect when numerically simulating the THz generation efficiency. Instead, we propose a new maximum efficiency as follows. The spectral frequency shift of an excitation pulse is reflected in the generation efficiency of a THz pulse that obeys the energy conservation rule in the $\chi^{(2)}$ process. Because this frequency shift results in the spectral broadening of the excitation pulse, the SRS process starts to be enhanced when the spectral shift of the excitation pulse approaches the lowest A-mode phonon frequency of 7.4 THz. Once the SRS process becomes dominant, THz pulse generation through optical rectification becomes greatly suppressed owing to the very large GVD in $LiNbO_3$. Then the maximum energy conversion efficiency can be considered to be (frequency of phonon) / (frequency of excitation pulse) = 1.9% in the case of 780 nm optical excitation. In this context, a laser with lower frequency, such as an Yb-doped laser, may realize more efficient optical rectification. This will also reduce the effect of GVD, meaning that the excitation pulse will be less stretched, resulting in enhanced efficiency. THz pulse generation using an Yb-doped laser has already been demonstrated [26, 28, 29], in which the amount of spectral modulation via the SRS process was found to be small. Very recently, a conversion efficiency of 0.28% has been experimentally demonstrated using intense Yb:YAG lasers with 1.3 ps pulse duration [30].

4. Conclusions

We experimentally demonstrated intense THz electric pulse generation with optical rectification in $LiNbO_3$ with the highest ever reported energy conversion efficiency of 0.21%. Bandwidth control of the optical excitation pulse suppresses the SRS process, leading to efficient THz pulse generation without the undesired energy dissipation of the excitation pulse. This is expected to provide new optimized conditions for extremely intense and high-efficiency THz pulse generation.

Acknowledgments

This work was supported by Industry-Academia Collaborative R&D from Japan Science and Technology Agency (JST) and a Grant-in-Aid for Scientific Research on Innovative Areas (No. 2210901 and No. 20104007) from the Ministry of Education, Culture, Sports, Science and Technology (MEXT) of Japan.

#162439 - $15.00 USD Received 2 Feb 2012; revised 1 Mar 2012; accepted 1 Mar 2012; published 5 Mar 2012